Energy and Power 2014, 4(1): 7-15
DOI: 10.5923/j.ep.20140401.02

Transesterification of Palm Oil by Using Silica Loaded Potassium Carbonate (K_2CO_3/SiO_2) Catalysts to Produce Fatty Acid Methyl Esters (FAME)

R. Irmawati[1,2,*], I. Shafizah[1], A. Nur Sharina[1], H. Abbastabar Ahangar[1,3], Y. H. Taufiq-Yap[1,2]

[1]Centre of Excellence for Catalysis Science and Technology, Faculty of Science, Universiti Putra Malaysia, 43400, UPM Serdang, Selangor, Malaysia
[2]Department of Chemistry, Faculty of Science, Universiti Putra Malaysia, 43400, UPM Serdang, Selangor, Malaysia
[3]Materials Science and Engineering Department, Islamic Azad University, Najafabad Branch, Najafabad 85141-43131, Iran

Abstract Transesterification of palm oil with methanol to form fatty acid methyl esters (FAME) was performed, using silica loaded with potassium carbonate, K_2CO_3/SiO_2 as a solid base catalyst. The catalyst was prepared by an impregnation method and calcined at 1237 K. The prepared catalysts were characterized by X-ray diffraction (XRD), Brunauer – Emmett - Teller (BET) surface area analysis, scanning electron microscopy (SEM), and temperature-programmed desorption of carbon dioxide (CO_2-TPD). High yield biodiesel (98.10%) was obtained with a reaction time of 3 h, reaction temperature of 333 K, molar ratio methanol to oil of 20:1, catalyst loading of 20 wt%, and catalyst amount of 4 wt%. Proton nuclear magnetic resonance (^{1}H-NMR) confirmed the existence of FAME with distinct peaks equivalent to hydrogen singlet from the methyl ester methoxyl group at 3.67 ppm and from methylenic hydrogen at 2.31 ppm. FAME was also successfully quantified using gas chromatography (GC) where peaks corresponded to fatty acid methyl esters of palm oil.

Keywords Biodiesel, Transesterification, Base catalyst, Palm oil

1. Introduction

Awareness of environmental protection encourages many researchers to study in biodiesel production as an alternative to fossil fuels. Fossil fuel can give negative impact on the environment through carbon oxides emissions, unburned hydrocarbons, sulphur dioxide and particulates [1,2,3,4]. Biodiesel can minimize greenhouse gas emissions because carbon dioxide from biodiesel combustion is offset by the carbon dioxide sequestered while growing oil palm or other feedstock [5]. Biodiesel usually obtained from vegetable oil such as palm oil [6], soybean oil [7], canola oil [8], and rapeseed oil [9] or sometimes from animal fats [10] by transesterification (Scheme 1) and molecules in biodiesel are primarily known as Fatty Acid Methyl Esters (FAME). Triglyceride are the composition of vegetable oils and animal fats, which are esters containing three free fatty acids. During transesterification, triglycerides are reacted with methanol which is low molecular weight alcohol to produce methyl esters of fatty acids and glycerol.

Triglycerides to methyl esters in complete reaction involves three sequential reactions with a monoglyceride (MAG) and a diglyceride (DAG) as intermediates. During transesterification, triglycerides (TAG) in the oil react with alcohol in the presence of a catalyst such as sodium hydroxide, NaOH or potassium hydroxide KOH to produce biodiesel. Transesterification occurs in three sequential reversible steps: (a) TAG reacts with methanol to produce a diglyceride (DAG), liberating a single fatty acid methyl ester, (b) DAG reacts with methanol to produce a monoglyceride (MAG) and another FAME, and (c) MAG reacts with methanol to produce a FAME, liberating the glycerol by-product. However, MAG and DAG are formed and remain in the final biodiesel product [11].

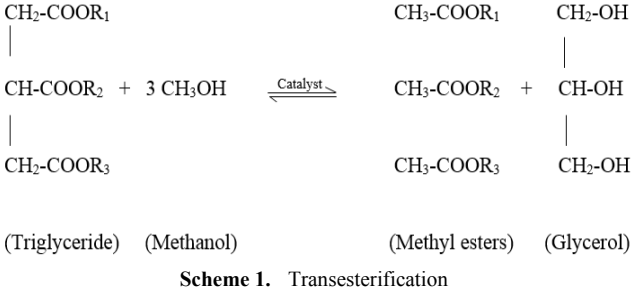

Scheme 1. Transesterification

Biodiesel produced by transesterification of vegetable oil with methanol is possible with both homogeneous acid or base catalyst and heterogeneous acid, base, or enzymatic

* Corresponding author:
irmawati@upm.edu.my (R. Irmawati)
Published online at http://journal.sapub.org/ep

catalysts [12, 13]. The base catalysts are more often used commercially than acid catalysts, which are corrosive. The development of the heterogeneous catalyst alleviates most of the economic and environmental weaknesses of the homogeneous catalyst problems such as the neutralization of the base catalyst during reaction and the difficulties when washing and separating the final product which will produce large amounts of wastewater [14,15].

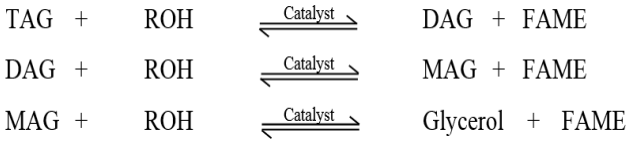

Scheme 2. Three consecutive reactions during transesterification

Ideal heterogeneous catalysts are highly stable and mesoporous, have strong active sites and a low cost [16]. A common technique to prepare heterogeneous catalyst is impregnation method which very simple, clean and environmentally friendly process. The development of a solid catalyst loaded on a support or carrier and can be called as impregnated catalyst, is very promising with good conversion results in the transesterification of vegetable oil. Previous research includes, K_2CO_3/Al-O-Si aerogel catalyst [3], F/CaO [14], and KOH supported on palm shell activated carbon catalysts [17]. Catalyst support with porous materials are favoured due to their high surface [2]. Other heterogeneous catalysts that showed good performance in the transesterification of vegetable oil are Na/NaOH/γ-Al_2O_3 [7], commercial hydrotalcite [18], zeolites and modified zeolites [19, 20] but complicated preparation has limited their industrial applications.

Transesterification of vegetable oils catalysed by various heterogeneous catalysts have been developed. Silica loaded with base metal salts or different potassium compounds are efficient solid-base catalysts [21]. K_2CO_3/Al-O-Si aerogel catalyst prepared by the sol-gel method exhibits good activity with a high yield of over 92%. However undesired leaching of the active components was also observed [3]. It was found that the K_2CO_3 catalyst exhibited much higher performance, proving that potassium plays different roles in catalysis. Pure K_2CO_3 proved to be remarkably active in biodiesel production by transesterification of sunflower oil with 90% conversion of oil in 108 min [22].

This work aims to produce biodiesel through a heterogeneous system with silica loaded potassium carbonate as a solid base catalyst in the transesterification of palm oil. The catalyst was prepared by impregnation method. To study the physicochemical properties of the catalyst prepared by X-ray Diffraction (XRD), Brunauer – Emmet - Teller (BET) surface area, Scanning Emission Microscopy (SEM), and Temperature Programmed Desorption of Carbon Dioxide (CO_2-TPD). The product will be analysed by ^{1}H-Nuclear Magnetic Resonance (^{1}H-NMR) to confirm the existence of biodiesel and Gas Chromatography (GC) to determine composition of methyl esters.

2. Materials and Method

2.1. Materials

Refined palm oil was purchased from Giant Hypermarket, Malaysia and all chemicals such as potassium carbonate (99.99%), silica (99.99%), and methanol were obtained from Merck, Germany. The given properties of silica were pore size of 100 Å and surface area 330 m^2/g, making it suitable for use as a catalyst support.

2.2. Methods

2.2.1. Catalyst Preparation

The catalysts were synthesized by using a wet impregnation method. Potassium carbonate powder, K_2CO_3 was mixed with 10 mL deionized water to form a K_2CO_3 solution. The solution was poured onto 5 g silica which acted as a support for the catalyst with weight percentage of 5 wt%. The mixture was stirred for 30 min. The solids were dried overnight in an oven at 373 K and calcined in air at 1273 K for 4 h. The calcined catalyst was then crushed into powder and sieved. The preparation process was repeated for other catalyst loadings of 10 wt%, 15 wt%, and 20 wt% K_2CO_3/SiO_2.

2.2.2. Catalyst Characterization

The crystalline phase of the catalyst was assessed by X-ray diffraction (XRD) analysis using a Shimadzu XRD-600 Diffractometer by employing CuKα radiation (λ = 1.541 Å) generated by Philips glass diffraction x-ray tube broad focus 2.7 kW type, operated at ambient temperature (30 kV and 100 mA). The samples were scanned at a range of $2\theta = 10^o - 60^o$ with a scanning rate of 2^o/min. The obtained diffractograms were matched against the Joint Committee on Powder Diffraction Standards (JCPDS) PDF1 database version 2.6. The surface area of the samples were determined by the nitrogen (N_2) adsorption-desorption technique, using Thermo Finnigan Sorptomatic Instrument model 1900. The BET surface area was calculated and total pore volume was determined by the estimation from the N_2 uptake $P/P_o \rightarrow 1$. The morphology and surface structure of the sample (support and catalysts) were identified using SEM with LEO 1455 Variable Pressure scanning electron microscopy. The analysis was performed at an accelerated voltage of 20kV. The samples were coated with a thin layer of gold as the conducting material using a BIO-RAS sputter coater. Basicity of the catalysts was determined using CO_2-TPD analysis and was performed using Thermo Finnigan TPD/R/O 1100. For each experiment, 0.002 g of catalyst was pre-treated in nitrogen to remove all water vapour and any impurities in the pipeline, which was then heated up to 523 K at 30 K min^{-1}. The samples were cooled to adsorption temperature 300 – 450 K and loaded with carbon dioxide. Prior to analysis, the pre-treated samples were flushed with helium and heated up to 1173 K at 10 K min^{-1}.

2.2.3. Transesterification Reaction

Synthesized catalysts were tested for transesterification of palm oil. Commercial palm oil (cooking oil Cap Buruh) was used and the experiments were performed in 50 mL round bottom flasks with a water-cooled condenser. 5 g of palm oil, methanol (MeOH) to oil molar ratio of 20:1, catalyst amount of 4 wt% with 5 wt% K_2CO_3/SiO_2 was put into the round bottom flask. Reflux was performed at 333 K for 1 h. The experimental design consisted of five factors and four levels (Table 1). At the end of the reaction, the mixtures were centrifuged. Three phases formed, the upper layer was methanol, the middle layer was a mixture of biodiesel and little amount of glycerol, and the bottom layer was solid catalyst. The catalyst was easily removed after centrifugation. Methanol was then removed from the biodiesel mixture by heating the mixture at 343 K for 1h to completely evaporate the methanol. The biodiesel mixture was left overnight for self-separation of biodiesel from glycerol. A separating funnel was used, resulting in an upper layer of biodiesel and bottom layer of glycerol. The biodiesel obtained was analyzed using ^{1}H-nuclear magnetic resonance (^{1}H-NMR) and gas chromatography (GC).

Table 1. Factors and their levels employed in orthogonal array

Factors	Levels
Reaction time	1 h, 3 h, 5 h, 7 h
Reaction temperature	333 K, 343 K, 353 K, 373 K
MeOH:oil molar ratio	20:1, 25:1, 30:1, 35:1
K_2CO_3 loading	5wt%, 10wt%, 15wt%, 20wt%
Catalyst amount	4wt%, 6wt%, 8wt%, 10wt%

3. Results and Discussion

3.1. Characterization of the Catalyst

3.1.1. X-ray Diffraction (XRD)

The XRD pattern of SiO_2 support (Figure 1) shows three main peaks at $2\theta = 20.31^o$, 21.50^o, and 35.5^o which correspond to (100), (002), and (110) planes, respectively. All of these peaks are well matched to the reference peaks from SiO_2 references peaks from SiO_2 JCPDS file no. 18-1169. However, the peak at $2\theta = 23.01^o$ is not clearly seen. This is due to the semicrystalline nature of the calcined SiO_2 support resulting from the irregular arrangement of atoms and/or molecules. Impregnating the pure SiO_2 solid with 5wt% K_2CO_3 produced the effective progressive increase in the degree of crystallinity of the above mentioned phase and intensity. The appearance of peak at $2\theta = 23.01^o$ is proportional to the amount of K_2CO_3. The presence of K_2CO_3 was observed according to the JCPDS file no. 01-07-0292.

Table 2 lists the full width at half maximum (FWHM) values of the catalyst corresponding to $2\theta = 21.50^o$ of the (002) plane. It is found that the FWHM values increases with K_2CO_3 loading. It can be seen from Figure 1 that the peak intensity decreases suggesting that at low loadings, K_2CO_3 might be mainly residing on the catalyst surface. With increased amounts, K_2CO_3 might also be incorporated into the SiO_2 lattice causing disarray in the support atomic arrangement. The K_2CO_3 not only disrupts SiO_2 crystallinity but also affects the size of the particles. The crystallite sizes of K_2CO_3/SiO_2 corresponding to $2\theta = 21.50^o$ were 82.39, 58.96, 51.51, and 30.71 nm with K_2CO_3 loadings of 5, 10, 15, and 20 wt% K_2CO_3/SiO_2, respectively. The crystallite size of SiO_2 was calculated by using the Debye-Scherrer formula:

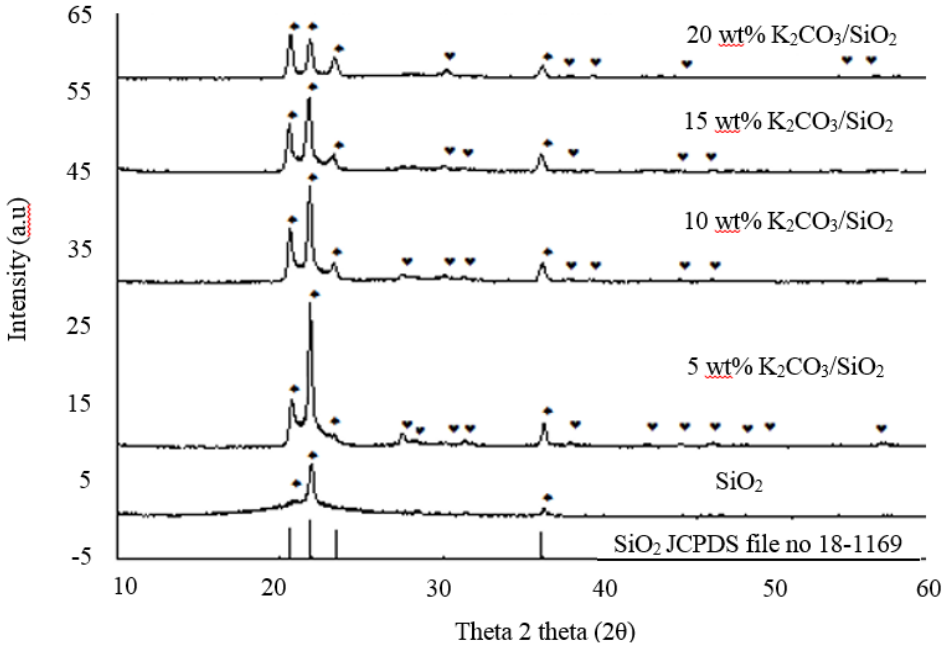

Figure 1. X-ray patterns of SiO_2 and K_2CO_3 supported SiO_2 catalysts (♥ K_2CO_3 (♦) SiO_2

$$t = \frac{0.89\lambda}{\beta_{hkl} \cos \theta_{hkl}} \quad (1)$$

Where

t = crystallite size for the (hkl) phase

λ = X-ray wavelength of radiation for CuKα (1.5438 Å)

β_{hkl} = full-width at half maximum (FWHM) at the (hkl) peak

θ_{hkl} = diffraction angle for the (hkl) phase

Table 2. XRD data for all catalysts

Catalyst	FWHM[a] 002/°	Crystallite size[b] (002)/nm	I_{002}[c]
5wt% K_2CO_3/SiO_2	0.1312	82.39	3.19
10wt% K_2CO_3/SiO_2	0.2400	58.96	0.93
15wt% K_2CO_3/SiO_2	0.2000	51.51	1.50
20wt% K_2CO_3/SiO_2	0.3200	30.71	1.14

[a] FWHM of (002) reflection
[b] Crystallite size by means of Scherrer's fomula
[c] Intensity of (002) reflection planes

3.1.2. BET Surface Area Measurement

The BET surface area, pore volume, and pore diameter of the supported catalysts are presented in Table 3. As shown in the table, the BET surface area of unsupported SiO_2 is 333.3 m^2/g. However, the surface area decreases significantly to 71.9, 37.2, 28.1 and 12.3 m^2/g for 5, 10, 15, 20 wt% of K_2CO_3 loading, respectively. The BET surface area values further decreased when the samples were calcined, in which 0.53, 0.49, 0.45, and 0.40 m^2/g were obtained for 5, 10, 15, 20 wt% supported samples, respectively. The huge differences in the BET surface area values for the calcined samples as compared to the uncalcined ones are due to the granulation of the originally powdery solid when the samples were calcined at high temperatures.

Table 3. Surface area, pore diameter, and pore volume for silica and K_2CO_3/SiO_2 for (A) before calcination and (B) after calcination

	Surface area (m^2 g^{-1})		Pore diameter (nm)		Pore Volume (cm^3 g^{-1})	
	A	B	A	B	A	B
SiO_2	333.3	-	8.8	-	0.7	-
5wt% K_2CO_3/SiO_2	71.9	0.53	33.7	30.5	0.6	0.0041
10wt% K_2CO_3/SiO_2	37.2	0.49	51.0	31.9	0.5	0.0039
15wt% K_2CO_3/SiO_2	28.1	0.45	53.7	32.0	0.4	0.0033
20wt% K_2CO_3/SiO_2	12.3	0.40	60.8	32.1	0.2	0.0030

As can be seen in Table 3, the pore volume of the catalysts ranged from 0.0030-0.0041 cm^3 whereas the pore size diameter ranged from 30.5 to 32.1 nm. According to Fernandez *et al*., (2007) [22], they defined that the diameter of triglyceride molecules (around 2 nm), as the diameter of the smallest cylinder where the molecule can pass without distortion. All of the catalysts synthesized in this study could easily accommodate the bulky triglyceride. Furthermore, the presence of K_2CO_3 on the surface and in the voids allows for sufficient contact between the reactant and the catalyst's active sites. There may also be some very small pores that cannot be occupied by triglycerides [23].

3.1.3. Scanning Electron Microscopy (SEM)

Details of the surface morphology of the K_2CO_3/SiO_2 catalyst were obtained from scanning electron microscopy (SEM) with magnification of 3000x and at a scanning voltage of 15kV are shown in Figure 2. All of the supported catalysts showed similar morphology and there is no particular shape can be derived from the image except for the rough surfaces of the materials. The images also shows K_2CO_3 (◆) were well distributed on SiO_2.

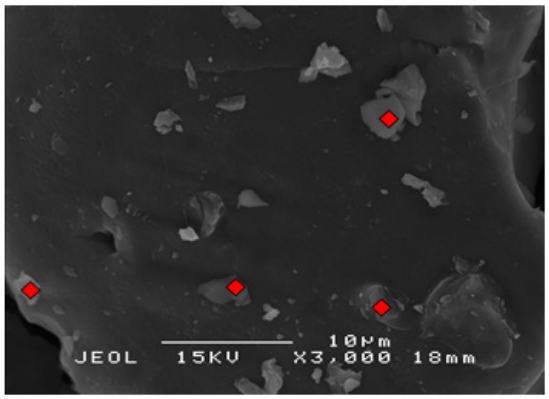

Figure 2(a). SEM micrograph of 5 wt% K_2CO_3/SiO_2

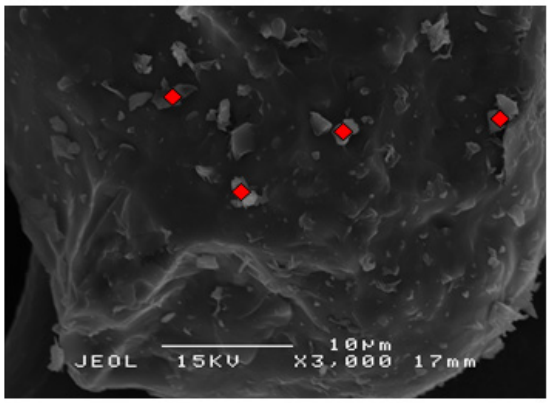

Figure 2(b). SEM micrograph of 10 wt% K_2CO_3/SiO_2

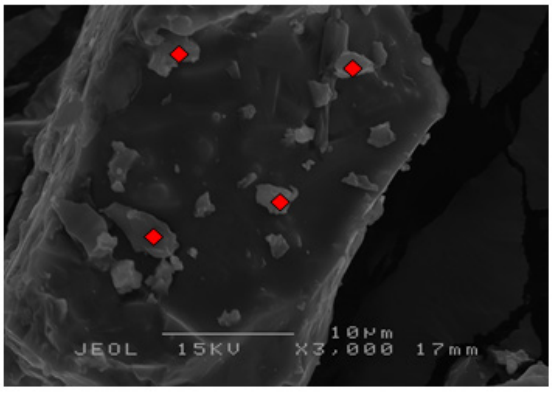

Figure 2(c). SEM micrograph of 15 wt% K_2CO_3/SiO_2

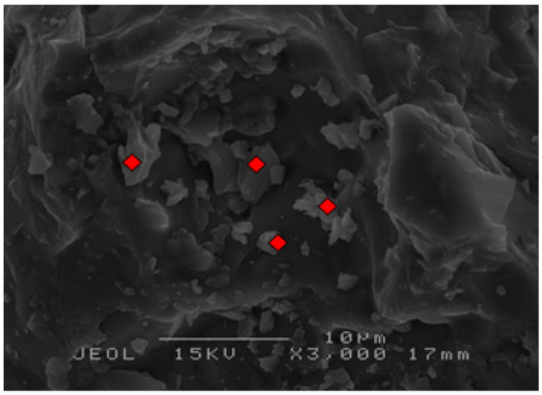

Figure 2(d). SEM micrograph of 20 wt% K_2CO_3/SiO_2

3.1.4. Temperature Programmed Desorption of Carbon Dioxide (CO_2-TPD)

The basicity of the catalyst was evaluated using CO_2-temperature programmed desorption (CO_2-TPD). Figure 3 shows the CO_2-TPD profiles of K_2CO_3/SiO_2 catalysts. The CO_2-TPD curves demonstrate the base strength of K_2CO_3-supported silica with different weight percentages. The quantification of desorbed CO_2 is accomplished by calculating the area under the peak and the amount obtained for each sample (Table 4).

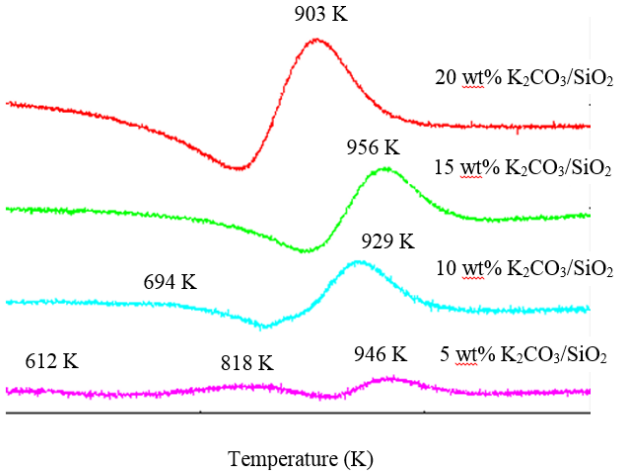

Figure 3. CO_2-TPD profiles of catalyst with different K_2CO_3 loading

The strength of basic sites was deduced from the work by Pasupulety et al., (2013) [24], where it was suggested that desorption temperature between 673-873 K indicates basic sites of weak and medium strength, and desorption temperature range of 873-1123 K indicates strong basic sites. According to Figure 3, it was discovered that 5 wt% K_2CO_3/SiO_2 catalyst produces a strong base as stipulated by the high desorption temperature of more than 600 K. In this study, the differences in the distribution of basic sites for each catalyst indicates that the basicity and base strength distributions are significantly influenced by the amount of K_2CO_3 loading on SiO_2. Figure 3 also revealed that the loading of 5 wt% K_2CO_3 on SiO_2 results in the creation of a large number of basic sites of weak and medium strength at T_{max} 612, 818, and 946 K. High amounts of K_2CO_3 (15 wt% and 20 wt%) increases the basic strength as the strong basic sites were revealed again by 10wt% K_2CO_3/SiO_2 at T_{max} = 694, and 929 K. Hence, high desorption activation energy is needed i.e 109.5 and 145.4 kJ/mole respectively.

From Table 4, it can be seen that the total amount of CO_2 desorbed increases from $1.6x10^{20}$, $1.9x10^{20}$, $4.1x10^{20}$, and $9.6x10^{20}$ atom/g with increased amounts of K_2CO_3; 5, 10, 15, and 20wt% K_2CO_3/SiO_2, respectively. It is noteworthy that the amount of carbon dioxide molecules available thermally was directly proportional to the K_2CO_3 loadings. It is possible that more active basic sites are present in the supported catalysts and therefore, there would be a higher availability of carbon dioxide that could be thermally desorbed. The order of basicity was as follows: 20wt% K_2CO_3/SiO_2 > 15wt% K_2CO_3/SiO_2 > 10wt% K_2CO_3/SiO_2 > 5wt% K_2CO_3/SiO_2. The trend suggests that higher K_2CO_3 loading in the case of silica-supported catalyst would achieve higher activity and selectivity in biodiesel production. This phenomenon indicated that the basicity of the catalysts became stronger as was reported by previous studies, Gao et al., (2008) [25] and Jing et al., (2004) [26]. The enhanced basic sites of the catalysts enabled high yield reactions to occur.

As was previously discussed, the number of basic sites were quantified by the integration of the desorption curves (Figure 3), which is proportional to the number of moles of CO_2 desorbed from the surface, which in turn is proportional to the number of monolayers. As reported by Zãvoianu et al., (2001) [27], desorbed CO_2 would increase the basicity, which would also increase the number of monolayers. It was reported that supported samples with a monolayer of the active phase generally has a higher number of adsorption sites per weight of active phase. This is attributed to the higher dispersion of the active phase and its interaction with the support. In this study, the number of monolayers increased by 0.8, 0.9, 1.8, and 4.3 as the loading of K_2CO_3 on the support increased from 5, 10, 15, and 20 wt% respectively.

3.2. Analysis of Biodiesel

3.2.1. ^{1}H-Nuclear Magnetic Resonance (^{1}H-NMR)

^{1}H-Nuclear Magnetic Resonance (^{1}H-NMR) was used to quantify fatty compounds in biodiesel based on the fact that the amplitude of a proton nuclear magnetic resonance (^{1}H-NMR) signal is proportional to the number of hydrogen nuclei contained in the molecule [28]. Figure 4 shows the spectrum of the biodiesel obtained at optimum condition by using K_2CO_3/SiO_2 catalyst. However, without using K_2CO_3/SiO_2 catalyst, biodiesel cannot be produced. The signal for methylene protons appears at 2.3 ppm which together with ester group in triglycerides. After transesterification, the methoxy protons of methyl esters appear at 3.7 ppm (Figure 4 and Table 5), which describes the typical chemical structures related to the ^{1}H-NMR spectrum.

Peaks are noted for saturated structures. Most of the peaks

have a chemical shift if the resonance is between 0 and 5 ppm. Additionally, the resonance of the unsaturated structures are between 5 and 9 ppm (alkene proton between 5 and 7 ppm, and aromatic protons between 7 and 9 ppm). Peak areas are measured by electronic configuration of the response signals in a spectrum. The yield of methyl esters was determined by areas of the signals of methylene and methoxy protons, according to the following equation [29]:

$$Y_{FAME} = 100 \text{ x } \left(\frac{2A_{ME}}{3A_{CH\,2}}\right) \quad (2)$$

Where Y_{FAME} is the yield (in percentage) of methyl esters, A_{ME} is signal area of the equivalent hydrogen singlet from the methyl ester methoxyl group (strong singlet); A_{CH2} is the signal area from the methylenic protons. In addition, derivation of factor 2 and 3 from the fact that the methylene carbon possesses two protons and the alcohol (methanol derived) carbon has three attached protons. Confirmation of the existence of methyl esters in biodiesel can be determined by these two distinct peaks. Other observed peaks are at 0.85 ppm of terminal methyl protons, a strong signal at 1.26 ppm related to methylene protons and at 5.28 ppm due to olefinic hydrogen [30]. A broad superposition of triplets between 1.0 and 0.8 ppm might also be considered as it appears as the terminal methyl group.

Table 4. Total number of CO_2 Molecules from Each Catalyst by CO_2-TPD

Catalyst	T_{max} (K)	Desorption Activation Energy, E_d(kJ/mole)	Carbon dioxide Desorbed (µmole/g)	Carbon Dioxide Desorbed (atom/g)	*Coverage (atom/cm^2)	**Monolayers of CO_2 Desorbed
			5wt% K_2CO_3/SiO_2			
1	612	101.7	64.5	3.9 x 10^{19}	5.3 x 10^{14}	0.8
2	818	132.1	90.8	5.5 x 10^{19}		
3	946	151.8	117.6	7.1 x 10^{19}		
		Total Carbon Dioxide Desorbed		**1.6 x 10^{20}**		
			10wt% K_2CO_3/SiO_2			
1	694	73.6	155.6	9.4 x 10^{19}	6.0 x 10^{14}	0.9
2	929	149.3	163.9	9.9 x 10^{19}		
		Total Carbon Dioxide Desorbed		**1.9 x 10^{20}**		
			15wt% K_2CO_3/SiO_2			
1	956	109.5	673.6	4.1 x 10^{20}	1.3 x 10^{15}	1.8
		Total Carbon Dioxide Desorbed		**4.1 x 10^{20}**		
			20wt% K_2CO_3/SiO_2			
1	903	145.4	1597.6	9.6 x 10^{20}	3.0 x 10^{15}	4.3
		Total Carbon Dioxide Desorbed		**9.6 x 10^{20}**		

Surface area:
5wt% K_2CO_3/SiO_2 = 0.53 m^2 g^{-1}, 10wt% K_2CO_3/SiO_2 = 0.49 m^2 g^{-1}, 15wt% K_2CO_3/SiO_2 = 0.45 m^2 g^{-1}, 20wt% K_2CO_3/SiO_2 = 0.40 m^2 g^{-1}
* CO_2 coverage is calculated by dividing the total amount of CO_2 desorbed by the total surface area of samples
** The monolayer of CO_2 desorbed are calculated by dividing the CO_2 coverage by 7 x 10^{14} atom cm^{-2}

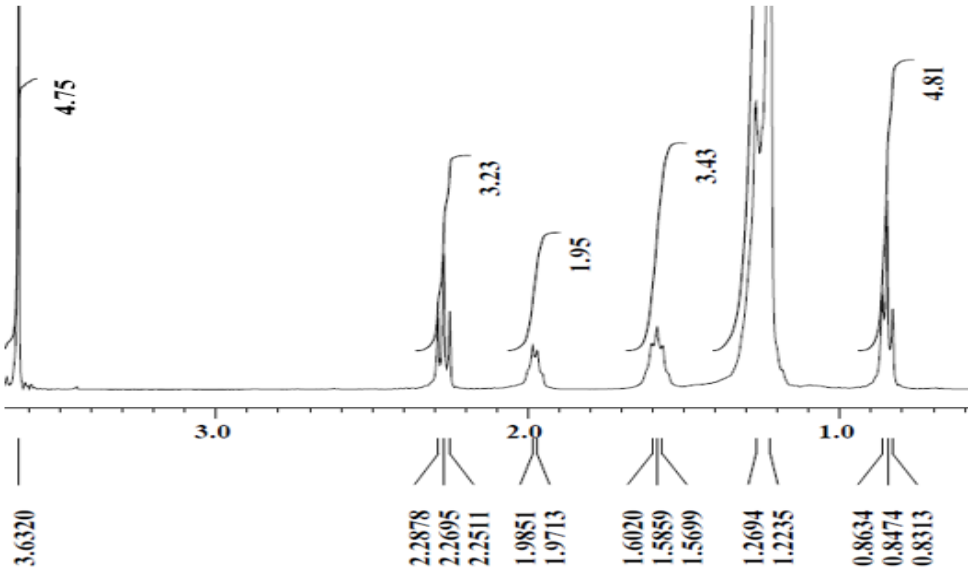

Figure 4. ^{1}H-NMR spectrum of biodiesel produced at reaction time 3 h, reaction temperature of 333 K, methanol to oil molar ratio of 20:1 with 20 wt% catalysts loading and 4wt% of catalyst amount

Table 5. Assignment of ^{1}H-NMR peaks of contained in biodiesel

Proton(s)	Functional group	Compound/ chemical shift, δ (ppm)
CH_3-C	Terminal methyl group	0.80 - 1.00
-(CH_2)n-	Backbone CH_2	1.22 - 1.42
-$CH_2CH_2COOCH_3$-	β-methylene proton	1.55 - 1.69
=CH-CH_2-	α-methylene group to one double bond	1.93 - 2.10
-CH_2COOR	α-methylene group to ester	2.31
-CO(CH_3)O	Methyl group to ester	3.67
-CH=CH-	Olefinic proton	5.27 - 5.41

Table 6. Fatty acid composition of biodiesel produced

Peak	Retention time (min)	Type	Unsaturated/Saturated Ratio	Percentage of ester (%)
1	1.8150	Saturated	C12:1 Laurate acid	0.3
2	2.246	Saturated	C14:0 Myristate acid	0.8
3	3.059	Saturated	C16:0 Palmitate acid	28.2
4	3.692	Monounsaturated	C17:0 Heptadecanoic acid	27.0
5	4.513	Internal standard	C18:0 Stearic acid	2.7
6	4.806	Monounsaturated	C18:1 Oleate acid	32.6
7	5.313	Polyunsaturated	C18:2 Linoleate acid (ω6)	8.3
8	6.171	Polyunsaturated	C 18:3 α-linoleate acid (ω2)	0.2

3.2.2. Component Determination in the Biodiesel by Gas Chromatography (GC)

The synthesized biodiesel products were analysed by gas chromatography to determine the composition of fatty acid methyl esters (Figure 5). Each peak corresponds to a fatty acid methyl ester component of palm oil and was identified using the library match software. The identities of the fatty acid methyl esters (FAME) were verified by comparing the respective retention time data with mass spectroscopic analysis.

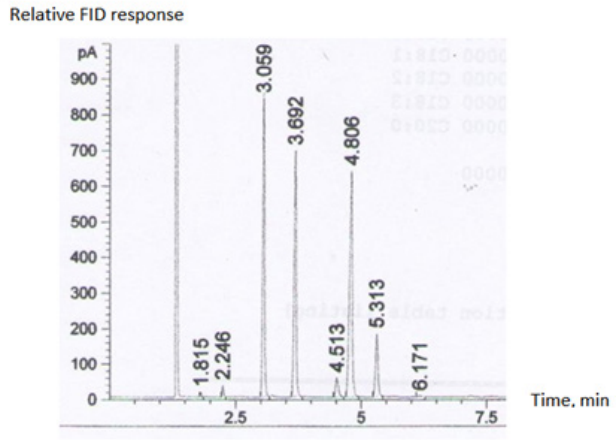

Figure 5. Chromatogram analysis for biodiesel produced at reaction time 3 h, reaction temperature of 333 K, methanol to oil molar ratio 20:1, with 20wt% catalyst loading and 4wt% of catalyst amount. FAME: C12 = methyl laureate; C14 methyl myristate; C16: methyl palmitate; C18 (C18:2 methyl linoleate; C18:1 methyl oleate; C18:0 methyl stearate)

The presence of three saturated and two unsaturated FAMEs in palm oil by GC analysis confirmed as they having similar impact spectra. FAME was in the range of 4 – 6 min [22]. Table 6 presents the results obtained for the biodiesel samples. The main methyl esters for palm oil biodiesel are palmitate (C16:0) and oleate (C18:1). This data agrees with published literature [31, 32].

4. Conclusions

Silica loaded with K_2CO_3 catalyst was successfully prepared by the impregnation method and improved biodiesel production. The influence of the different K_2CO_3 loadings on silica, which was varied from 5, 10, 15, and 20 wt% were studied comprehensively. The addition of K_2CO_3 on SiO_2 significantly influenced the crystallinity of the supported catalyst but also affected the particle size of the catalyst, which was found to decrease with increased amounts of K_2CO_3. Additionally, BET surface area analysis revealed that K_2CO_3-supported SiO_2 has a small surface area but its high pore diameter allows it to accommodate bulky triglyceride molecules. According to the CO_2-TPD results, the addition of K_2CO_3 on SiO_2 results in the creation of strong basic sites which is needed as the basicity of the catalyst plays an important role in base-catalyzed biodiesel production which in this case 20wt % catalyst which has shown having the highest number of basic site which is determined as the prime contributor to the highest activity for the transesterification reaction as opposed to other

loadings.

The transesterification reaction of palm oil catalyzed by silica loaded with K_2CO_3 prepared in this study revealed the efficiency of the catalyst for the reaction. It was found that up to 98.10% yield of biodiesel was obtained when palm oil was transesterified with methanol in the presence of K_2CO_3/SiO_2 catalysts. The existence of the biodiesel was confirmed by ^{1}H-NMR analysis in which the distinct peaks of methyl esters methoxyl group at signal 3.67 ppm, α methylene groups of esters at signal 2.31 ppm and methyl ester compositions were successfully quantified.

ACKNOWLEDGEMENTS

This research was supported by Graduate Research Fellowship (GRF). The authors gratefully acknowledge the contribution from Malaysian Palm Oil Board (MPOB) for helping with the yield analysis.

REFERENCES

[1] M. Balat and H. Balat, 2010. Progress in biodiesel progressing. *Applied Energy* 87, 1815-35.

[2] Zuraida Wan and B. H. Hameed, 2011. Transesterification of palm oil to methyl ester on activated carbon supported calcium oxide catalyst. *Bioresource Technology*, 102, 2659-2664.

[3] Lukić I., Krstić J., Jovanović D., and Skala D., 2009. Alumina/silica supported K_2CO_3 as a catalyst for biodiesel synthesis from sunflower oil. *Bioresource Technology*, 100, 4690-4696.

[4] Martin S. Gross, Maria A. Ulla, and Carlos A. Querini, 2009. Catalytic oxidation of diesel soot: New characterization and kinetic evidence related to the reaction mechanism on K/CeO_2 catalyst, 1360, 81-88.

[5] L. lin, Cunshan Z., Vittayapadung S., Xiangqian S., and Mindong D., 2011. Opportunities and challenges for biodiesel fuel. *Applied Energy,* 88, 1020-1031.

[6] Zabeti M., Wan Daud W.MA., and Aroua M.K., 2009. Activity of solid catalysts for biodiesel production: A review. *Fuel Processing Technology*, 90, 770-7.

[7] Kim H., Kang B., Kim M., Park Y., Kim D., Lee J., and Lee K., 2004. Transesterification of vegetable oil to biodiesel using heterogeneous base catalyst. *Catalysis Today*, 93, 315-1330.

[8] D'Cruz A., Kulkarni M.G., Meher L.C., and Dalai A.K., 2007. Synthesis of biodiesel from canola oil using heterogeneous base catalyst. *Journal of the American Oil Chemist's Society*, 84, 937-943

[9] MacLeod C. S., Harvey A. P., Lee A. F., and Wilson, K., 2008. Evaluation of the activity and stability of alkali-doped metal oxide catalysts for application to an intensified method of biodiesel production. *Chemical Engineering Journal,* 135, 63-70.

[10] J.M. Encinar, N. Sámchez, G. Martínez, and L. García, 2011. Study of biodiesel production from animal fats with high free fatty acid content. *Bioresource Technology*, 102, 10907-10914.

[11] Freedman B., Butterfield R.O., and Pryde E.H., 1986. Transesterification kinetics of Soybean Oil, *Journal of the American Oil Chemist's Society*, 63, 1375-1380.

[12] Liu X.J., Piao X.L., Wang Y.J., Zhu S.L., and He H.Y., 2008. Calcium methoxide as a solid base catalyst for the transesterification of soybean oil to biodiesel with methanol. *Fuel,* 87, 1076-82.

[13] Bo X., Guomin X., Lingfeng C., Ruiping W., and Lijing G., 2007. Transesterification of palm oil with methanol to biodiesel over a KF/Al2O3 heterogeneous base catalyst. *Energy & Fuel*, 21, 3109-3112.

[14] Wen L., Wang Y., Lu D., Hu S., and Han H., 2010. Preparation of KF/CaO nanocatalyst and its application in biodiesel production from Chinese tallow seed oil. *Fuel*. 89, 2267-2271.

[15] Zhang L., Sheng B., Xin Z., Liu Q., and Su S., 2010. Kinetics of Transesterification of Palm Oil and Dimethyl Carbonate for Biodiesel Production at the Catalysis of Heterogeneous Base Catalyst. *Bioresource Technology*, 101, 8144-8150.

[16] Lotero E., Liu Y.J., Lopez D.E., Suwannakarn K., Bruce D.A., and Gooqwin Jr. J.G., 2005. Synthesis of biodiesel via acid catalysis. *Industrial & Engineering Chemistry Research,* 44, 5353-5363.

[17] Baroution S., M.K. Aroua, A.A.A. Raman, and N.M.N. Sulaiman, 2010. Potassium hydroxide catalyst supported on palm shell activated carbon for transesterification of palm oil. *Fuel Processing Technology*, 91, 1378-1385.

[18] Xie W., Peng H., and Chen L., 2006. Transesterification of soybean oil catalysed by potassium loaded alumina as a solid base catalyst. *Applied Catalysis A: General*, 257(2), 213-23

[19] Xie W., Huang X., and Li H., 2007. Soybean oil methyl esters preparation using NaX zeolites loaded with KOH as a heterogeneous catalyst. *Bioresource Technology*, 98(4), 936-939.

[20] Suppes G. J., Dasari M. A., Doskocil E. J., Mankidy P. J., and Goff M. J., 2004. Transesterification of soybean oil with zeolite and metal catalysts. *Applied Catalysis A: General*, 257(2), 213-223.

[21] BenjapornkulapongS., Ngamcharussrivichai C., and Bunyakiat K., 2009. Al_2O_3-supported alkali and alkali earth metal oxides for transesterification of palm kernel oil and coconut oil, *Chemical Engineering Journal,* 145, 468.

[22] Fernandez M. B., Tonetto G. M., Crapiste G., and Damiani D. E., 2007. Kinetic of the hydrogenation of sunflower oil over alumina supported palladium catalyst, *International Journal of Chemical Reactor Engineering*, 5, A10.

[23] Jacobson K., Gopinath R., Meher L. C., and Dalai A. K., 2008. Solid acid catalyzed biodiesel production from waste cooking oil. *Applied Catalysis B*, 85, 86-91.

[24] Pasupulety N., Gunda K., Liu Y., Rempel G.L., and Ng F.T.T., 2013. Production of biodiesel from soybean oil on CaO/Al_2O_3 solid base catalysts. *Applied Catalyst A: General*, 452, 189-202.

[25] Gao L., Xu B., Xiao G., and Lv J., 2008. Transesterification of palm oil with methanol to biodiesel over a KF/Hydrotalcite solid catalyst. *Energy and Fuels*, 22, 3531-3535.

[26] Jing Q., Lou H., Fei J., Hou Z., and Zheng X., 2004. Syngas production from reforming of methane with CO_2 and O_2 over Ni/SrO–SiO_2 catalysts in a fluidized-bed reactor. *International Journal of Hydrogen Energy,* 29, 1245–51.

[27] Zãvoianu R., Dias C. R., and Portela M. F., 2001. Stabilisation of β-$NiMoO_4$ in TiO_2-supported catalysts, *Catalysis Communications* 2, 1, 37.

[28] Satyarthi J.K., Srinivas D., and Ratnasamy P., 2009. Factors influencing the kinetics of esterification of fatty acids over solid acid catalysts. *Energy and Fuels*, 23, 2273-2277.

[29] Nakagaki S., Alesandro B., Vannia C.D.S., Victor H.R.D.S., Heron V., Fabio S. N., and Luiz P.R., 2008. Use of anhydrous sodium molybdate as an efficient heterogeneous catalyst for soybean oil methanolysis. *Applied Catalysis A: General,* 351, 267-274.

[30] Tariq M., Ali S., Ahmad F., Ahmad M., Zafar M., Khalid N., and Khan M.A., 2011. Identification FT-IR, NMR (1H and 13C) and GC/MS studies of fatty acid methyl esters in biodiesel from rocket seed oil. *Fuel Processing Technology*. 92, 336-341.

[31] Demirbas, A., 2003. Biodiesel fuels from vegetable oils via catalytic and non-catalytic supercritical alcohol transesterification and other methods: A survey, *Energy Conversion and Management*, 44, 2003, 2093-210.

[32] A. Ivanoiu, A. Schmidt, F. Peter, L.M. Rusnac and M. Ungurean, 2011. Comparative Study on Biodiesel Synthesis from Different Vegetables Oils. *Chemical Bulletin of "POLITEHNICA" University of Timisoara*, 56(70), 2.